

# Rubber-modified bone cement

A. MURAKAMI

*Department of Chemical Engineering, Himeji Institute of Technology, 2167 Shosha, Himeji, Japan 671-22*

J. C. BEHIRI, W. BONFIELD

*Department of Materials, Queen Mary College, London E1 4NS, UK*

A precursor rubber-toughened polymethyl-methacrylate (PMMA) powder developed by ball-milling was incorporated into a series of test bone cements, with different combinations of PMMA powder, rubber-toughened PMMA powder, MMA monomer and benzoyl peroxide (BPO) initiator. The resulting microstructures were characterized by electron microscopy and measurements made of the tensile properties, fracture mechanics parameters and curing features. It is demonstrated that rubber-toughened PMMA powder additions give a significant increase in elongation and fracture toughness, with a reduction in setting time.

## 1. Introduction

Acrylic bone cement is an important component of the total hip replacement procedure in orthopaedic surgery [1]. In a typical operation, a metallic stem is secured in the medullary cavity of the femur by an *in situ* polymerization of the bone cement and located in an ultra-high molecular weight polyethylene acetabular cup. While various combinations of alloys, ceramics and polymers have been utilized in the past twenty years as stems and cups, polymethyl methacrylate (PMMA) has remained as an almost universal choice for bone cement. The considerable clinical success obtained with total hip replacement in elderly patients, with 90% achieving a prosthesis lifetime of 10 years or more, certainly reflects on the relative ease with which PMMA can be mixed and inserted in the femoral cavity followed by its relatively short setting time ( $\sim 8$  min). Against these advantages should be balanced the exothermic nature of the polymerization which generates a local temperature maximum of  $110^\circ\text{C}$  with associated bone necrosis, together with a reduced blood pressure. In addition, in the longer term, the mechanical mismatch in the elastic deformation characteristics across the bone-cement-metal composite can result in fracture of the bone cement, with a consequent loosening of the implant. This process is accentuated by the tendency with time for bone resorption to occur at the interface in response to the presence of the relatively stiff metal stem.

Given the large number of total hip replacement operations performed annually ( $\sim 40\,000$  in the UK alone) then even a relatively small failure rate of 10% has important implications in terms of the need for revision operations. When to this number is added the unsatisfied need for *long-term* total hip replacement procedures in younger patients and for other joints such as the knee, then it is readily apparent that improvements in the properties of bone cement would have far-reaching consequences. There are in fact two major research initiatives in progress: first, to elim-

inate cement completely by developing either bone ingrowth into a porous metal stem or bone apposition at a bioactive surface [2] and second, to reduce the exotherm and/or improve the fracture toughness of existing acrylic bone cement. All these approaches will if successful increase the spectrum of procedures for joint replacement. This paper is concerned in particular with an investigation of the effects of rubber modification of bone cement as a means of increasing fracture toughness.

Previous approaches to enhancing the mechanical properties of bone cement have included fibre reinforcement [3-6]. However, the resultant increase in stiffness in the fibre reinforcement cement can adversely affect the distribution of load from the metal stem to the surrounding bone [5]. For this reason the lower strengthening efficiency in a particulate composite allows a better mechanical match with the surrounding materials [2]. Of particular current interest is the toughening of PMMA with rubber particles (RTPMMA) [7-11] and the development of a transparent composite (either by matching the refractive indices of matrix and filler or by reducing the size of the particles to less than the wavelength of light ( $\sim 0.2\ \mu\text{m}$ )) [12, 13]. In these studies the particles were shown to have a spherical PMMA core surrounded by a rubbery inner shell of crosslinked copolymer (butylmethacrylate-styrene) and an outer shell forming the PMMA matrix [7, 10, 12]. It was demonstrated that this type of particle produces an enhanced toughness [7, 10, 11], which has been attributed to a mechanism of plastic shear and cavitation rather than crazing [7-11]. In the current study, this concept has been developed to establish the mechanical properties and morphology of a variety of rubber-toughened PMMA composites as potential bone cement materials.

## 2. Materials

Pellets of rubber-toughened PMMA, containing

TABLE I Chemical compositions of bone cements

Material	PMMA powder (g)	RTPMMA powder (g)	BPO (g)	MMA monomer* (g)
CMW†	40	0	1.2	20.724
40/0	40	0	0.6	20.724
30/0	30	0	0.6	20.724
20/10	20	10	0.6	20.724
15/15	15	15	0.6	20.724
10/20	10	20	0.6	20.724
0/30	0	30	0.6	20.724
0/20	0	20	0.6	20.724
0/15	0	15	0.6	20.724

\*Monomer contained N: N-dimethyl-*p*-toluidine (0.16 g), ethyl alcohol (0.196 g), ascorbic acid (0.004 g) and hydroquinone (0.0004 g).

†CMW bone cement (Type 1).

approximately 40 vol% of rubber particles (ICI Grade TD542), and acrylic bone cement (CMW Dentsply Ltd, PMMA powder and MMA monomer) were the starting materials. Rubber-toughened PMMA powder was then produced in the following procedure. First, the rubber-toughened PMMA pellets were dissolved in acetone and gave an insoluble fraction, consisting of rubber-PMMA particles [11, 14], which was extracted and crushed to a fine powder using a ball-mill with a water slurry. The rubber-toughened PMMA powder was subsequently dried in a vacuum chamber at 70°C and the < 70 µm fraction was separated from the dry powder using a sieve to give a particle size similar to that of the PMMA powder. From these starting powders, bone cements of different compositions were prepared, as shown in Table I. A standard commercial bone cement (CMW Dentsply Ltd) was prepared by mixing fixed amounts of PMMA powder, MMA monomer and a reaction initiator (benzoyl peroxide (BPO)) to provide a control. Modifications of this mixture with reduced weights of BPO (40/0) and PMMA powder (30/0), respectively, for a given weight of MMA monomer, were also developed. A further series of compositions in which rubber-toughened PMMA powder was substituted for PMMA powder in various weight fractions was then established (20/10, 15/15, 10/20). Finally, various amounts of rubber-toughened PMMA powder were incorporated directly into MMA monomer (0/15, 0/20, 0/30).

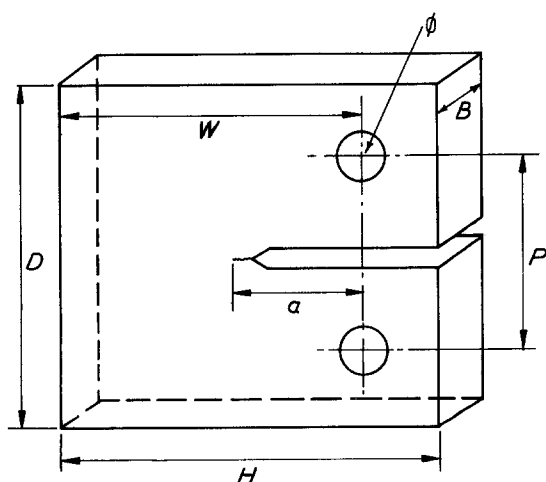


Figure 1 Schematic diagram of compact tension specimen.  $D = 33$  mm,  $H = 34$  mm,  $P = 18$  mm,  $\phi = 4.8$  mm,  $W = 26$  mm,  $B = 5$  mm.

### 3. Experimental procedure

Standard specimens for the tensile and fracture tests were compressed in aluminium moulds at 0.7 MN m<sup>-2</sup> pressure at 21 ± 1°C. The tensile test was performed in an Instron testing machine at a crosshead speed of 1 mm min<sup>-1</sup> using an extensometer to measure displacement.

Specimens for the compact tension (CT) test were machined to the dimensions shown in Fig. 1. A sharp crack was produced in the CT specimen by gently tapping a scalpel blade at the notch root. The CT specimens were tested in an Instron testing machine at a displacement rate of 1 mm min<sup>-1</sup> and the load-displacement curve was recorded. These mechanical tests were performed at room temperature (21 ± 1°C). The critical stress intensity factor,  $K_{Ic}$ , was calculated from

$$K_{Ic} = \frac{YPa^{1/2}}{BW} \quad (1)$$

where  $P$  = load at the crack initiation,  $a$  = crack length,  $B$  = thickness of specimen,  $W$  = width of specimen and  $Y$  = geometrical factor.  $Y$  is given by

$$Y = 29.6 - 185.5 \left( \frac{a}{W} \right) + 655.7 \left( \frac{a}{W} \right)^2 - 1017 \left( \frac{a}{W} \right)^3 + 638.9 \left( \frac{a}{W} \right)^4 \quad (2)$$

The procedures followed for the  $K_{Ic}$  measurements were according to the ASTM E-399 method. In addition, the strength ratio,  $R$ , was also determined, with  $R$  for the CT specimen given by

$$R = \frac{\sigma_{net}}{\sigma_y} = \frac{2P_{max}(2W + a)}{B(W - a)^2\sigma_y} \quad (3)$$

where  $\sigma_{net}$  = maximum net stress calculated by beam bending theory,  $\sigma_y$  = yield strength and  $P_{max}$  = maximum load.

In addition, dynamic mechanical thermal analysis (DMTA) was conducted to determine the influence of the ball-milling procedure, while the curing characteristics of the various test cements, which represent an important clinical property, were measured according to the ASTM F1451-81 procedure at 21 ± 1°C. The corresponding microstructures and fracture surfaces of the various test cements were assessed by scanning and transmission electron microscopy, the

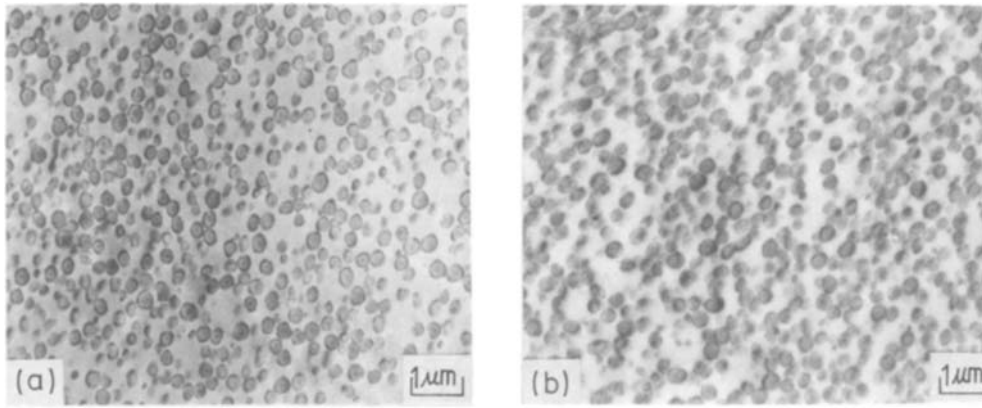


Figure 2 Transmission electron micrographs of rubber-toughened PMMA: (a) untreated, (b) ball-mill treated.

latter performed on microtomed sections following staining with osmium tetroxide.

## 4. Results

### 4.1. The effect of ball-milling

A typical TEM micrograph (Fig. 2a) shows that pellets, prepared by melt-blending the as-received rubber-toughened PMMA, contain particles of the order of  $0.3\ \mu\text{m}$  diameter. It can be seen that the particles have the characteristic cored structure, with a spherical centre. Rubber-toughened PMMA in powder form cannot be obtained from commercial sources at present. Therefore in the present study it

was necessary to crush rubber-toughened PMMA pellets into a fine powder as a precursor for the preparation of the test bone cements. Both rubber-toughened PMMA pellets and rubber-toughened PMMA powder obtained from the ball-milling were moulded at  $190^\circ\text{C}$  into test specimens to assess the effect of the additional ball-milling procedure on morphology and mechanical properties.

It was established that the microstructures (compared in Fig. 2) and the tensile properties (listed in Table II) of ball-mill treated rubber-toughened PMMA are not significantly different from those of as-received rubber-toughened PMMA. DMTA results

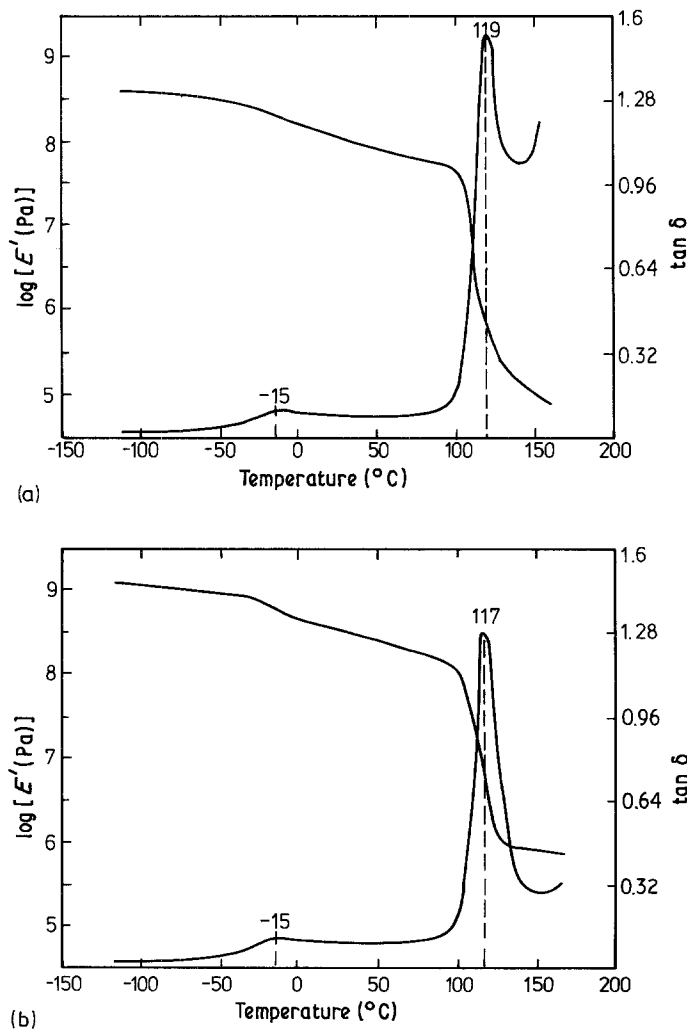


Figure 3 Temperature dependence of dynamic modulus  $E'$  and  $\tan\delta$  for rubber-toughened PMMA: (a) untreated, (b) ball-mill treated.

TABLE II Mechanical properties of rubber-toughened PMMA

Treatment	Young's modulus (GN m <sup>-2</sup> )	Yield strength (MN m <sup>-2</sup> )	UTS (MN m <sup>-2</sup> )	Elongation (%)
Untreated (original RTPMMA)	1.34 (0.09)*	31.3 (0.8)	31.8 (1.2)	29.9 (8.6)
Ball-mill treated	1.35 (0.08)	31.5 (0.5)	31.3 (0.7)	31.0 (7.2)

\*( ): standard deviation.

(Fig. 3) also show that the rubber peak of  $\tan\delta$  and  $T_g$  of the PMMA matrix are not affected by the ball-milling procedure. However, the ball-milled rubber-toughened PMMA does show an increased  $E'$  modulus at low temperature and the appearance of the rubbery plateau at high temperature.

#### 4.2. Tensile properties

The results of similar tensile tests obtained for a standard bone cement and the complete series of rubber-modified bone cements of different composition are listed in Table III. For the standard bone cement components, it can be seen in Fig. 4 that the reductions in PMMA powder and BPO amounts reduce the modulus and strength parameters while increasing the elongation to fracture. The effect of the mixing ratio of PMMA to rubber-toughened PMMA powder on the tensile properties of the bone cements is also illustrated in Fig. 4 and demonstrates a continuing decrease in the tensile modulus, yield strength and ultimate tensile strength with an increasing content of rubber-toughened PMMA powder, while the elongation increases markedly.

Table III also reveals that a complete substitution of rubber-toughened PMMA powder for PMMA powder gives a further significant increase in elongation, while the tensile modulus, yield stress and

ultimate tensile strength are reduced for a comparable mixture (i.e. 30/0 cf. 0/30). The various rubber-toughened PMMA powder-MMA monomer mixtures investigated did not show a significant variation in mechanical properties.

Stress whitening was observed during the tensile testing of all the rubber-toughened PMMA powder-containing bone cements.

#### 4.3. Microstructure

Typical transmission electron micrographs of bone cements containing a mixture of PMMA and rubber-toughened PMMA powder, and those containing exclusively rubber-toughened PMMA powder, are compared in Fig. 5. Both micrographs exhibit cored particles, with the difference that particle-free areas occur in the PMMA-rubber-toughened PMMA powder bone cements (Fig. 5a) in contrast to the homogeneous distribution noted in a rubber-toughened PMMA powder bone cement (Fig. 5b). A corresponding

TABLE III Mechanical properties of bone cements

Material	Tensile modulus (GN m <sup>-2</sup> )	Yield strength (MN m <sup>-2</sup> )	UTS (MN m <sup>-2</sup> )	Elongation (%)
CMW	3.65 (0.17)*	60.5 (1.1)	60.5 (1.1)	2.8 (0.4)
40/0	3.50 (0.28)	59.8 (2.1)	59.8 (2.0)	2.9 (0.4)
30/0	2.87 (0.07)	50.9 (1.1)	50.7 (1.0)	4.5 (1.8)
20/10	2.59 (0.14)	46.7 (1.3)	43.9 (1.8)	9.2 (5.9)
15/15	2.66 (0.21)	47.3 (2.8)	43.6 (3.1)	10.2 (3.1)
10/20	2.11 (0.10)	39.6 (0.6)	36.0 (1.9)	12.6 (6.8)
0/30	2.11 (0.07)	40.2 (0.8)	33.1 (0.9)	22.1 (6.4)
0/20	2.15 (0.16)	40.1 (3.8)	32.6 (2.6)	37.9 (10.4)
0/15	2.42 (0.08)	45.4 (2.4)	35.1 (1.4)	25.7 (11.4)

\*( ): standard deviation.

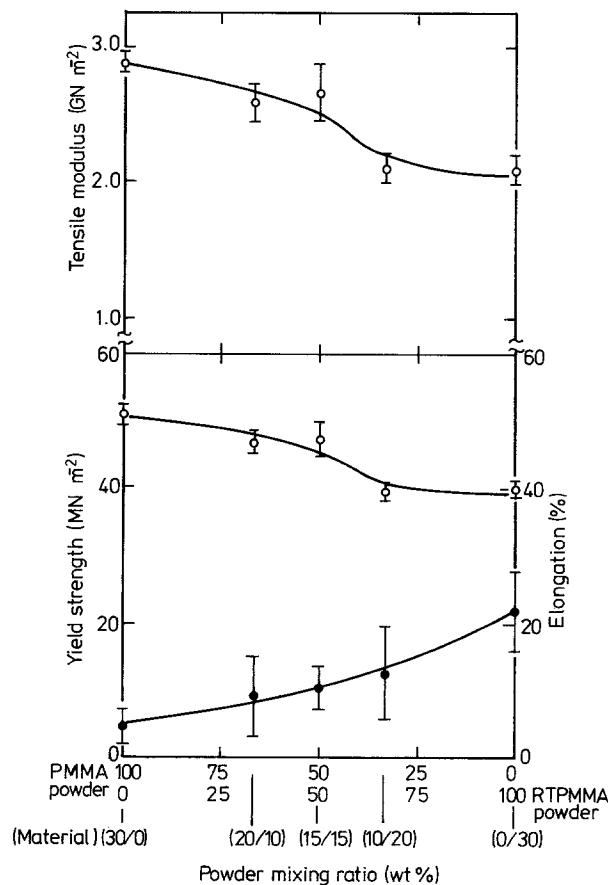


Figure 4 Effects of powder mixing ratio on the mechanical properties of rubber-modified bone cement. (○) Tensile modulus or yield strength; (●) elongation.

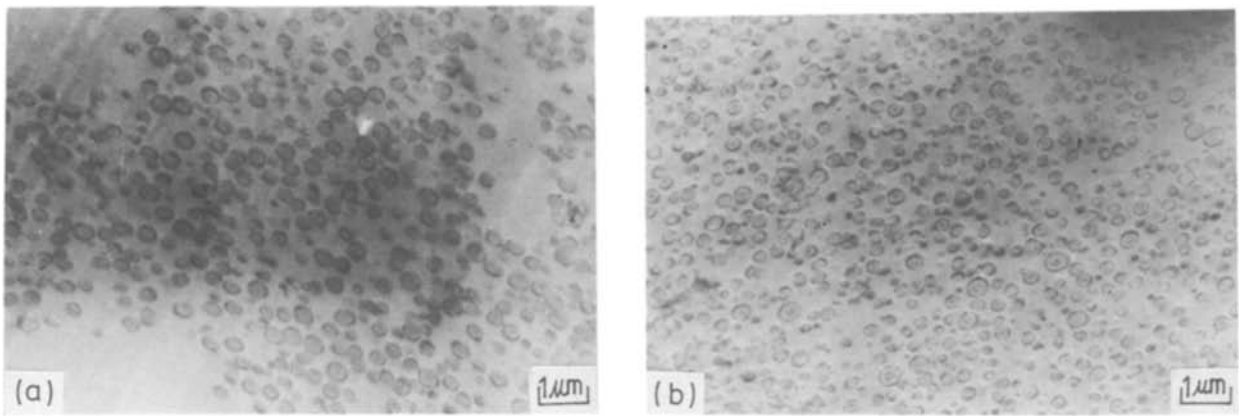


Figure 5 Transmission electron micrographs of rubber-modified bone cement: (a) 15/15, (b) 0/20.

micrograph (Fig. 6) from a “bulk” rubber-toughened PMMA specimen following tensile testing, taken from the region of stress whitening, shows dark lines (osmium tetroxide staining) perpendicular to the tensile direction indicative of crazing [15, 16].

#### 4.4. Fracture toughness and fractography

The results of fracture toughness measurements for the standard bone cement, and some selected modifications, indicate increases in  $K_c$  and  $R$  with an increase in the rubber-toughened PMMA powder content, which parallels the increase in elongation shown in Table IV.

The transition in fracture toughness gave different fracture surfaces. Relatively smooth fracture surfaces produced by a fast unstable fracture were observed for the standard bone cement and the 30/0 variant (Fig. 7). It should be noted that discrete PMMA particles can still be observed. In contrast, in all the rubber-toughened bone cements (i.e. PMMA powder–rubber-toughened PMMA powder and rubber-toughened PMMA powder alone) stable crack propagation, with associated stress whitening and ductile tearing, was noted, as shown in Fig. 8a for a 0/20 sample. At higher magnification (Fig. 8b), some holes created by particle–matrix debonding can be seen, together with some ovulation of the originally spherical particle geometry. The fracture process cul-

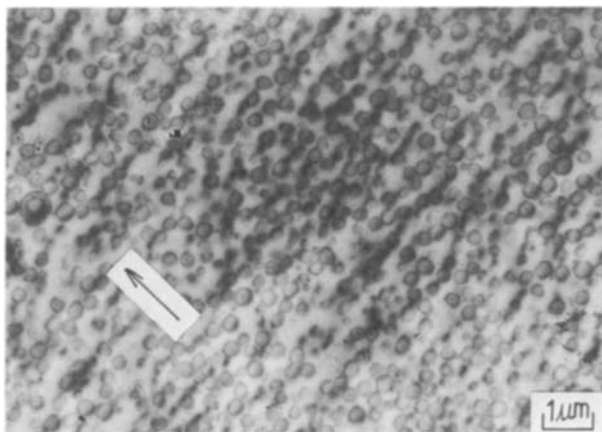


Figure 6 Transmission electron micrograph from a stress-whitened specimen of rubber-toughened PMMA. The arrow shows the tensile direction.

minated in an unstable fracture, but with a rougher surface profile than noted for the standard bone cement, as is shown in Fig. 9 for 0/20 and Fig. 10 for 15/15 samples.

#### 4.5. Curing characteristics

The curing characteristics of the standard and rubber-modified bone cements are shown schematically in Fig. 11, with the measured dough time, setting time and maximum temperature reported.

These parameters (Table V) are only directly comparable for a given amount of material. Hence the significant result is that an increase in the rubber-toughened PMMA powder content (e.g. 15/15 compared with 30/0) decreases the maximum temperature and, in particular, the setting time.

### 5. Discussion

The results demonstrate that the additional ball-milling procedure required to produce rubber-toughened PMMA powder as a precursor for bone cement does not degrade the mechanical properties. Indeed there may be some enhancement, perhaps attributable to crosslinking of the PMMA matrix by a mechanochemical reaction. The cored structure of the particles is associated with a spherical core of PMMA, a surrounding shell of rubbery crosslinked copolymer and an outer shell of PMMA.

With respect to the incorporation of rubber-toughened PMMA powder into bone cement, it was demonstrated that either in combination with PMMA

TABLE IV Fracture toughness and strength ratio of bone cements

Material	$K_c$ (MN m <sup>-3/2</sup> )	$\sigma_{net}$ (MN m <sup>-2</sup> )	$R = \sigma_{net}/\sigma_y$
CMW	1.84 (0.03)*	19.2 (0.3)	0.32
30/0	1.94 (0.16)	19.8 (1.3)	0.38
15/15	2.26 (0.07)	23.6 (0.7)	0.52
0/20	2.46 <sup>†</sup> (0.13)	25.7 (1.3)	0.64

\* ( ): standard deviation.

<sup>†</sup> Not plane-strain conditions.

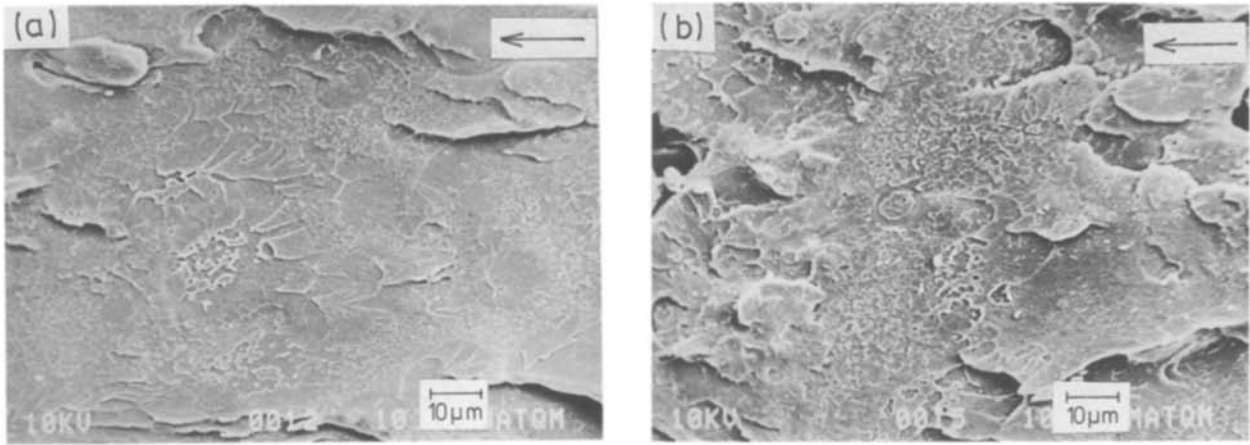


Figure 7 Scanning electron micrograph of fracture surfaces produced by unstable crack propagation: (a) CMW, (b) 30/0. The arrow shows the direction of crack propagation.

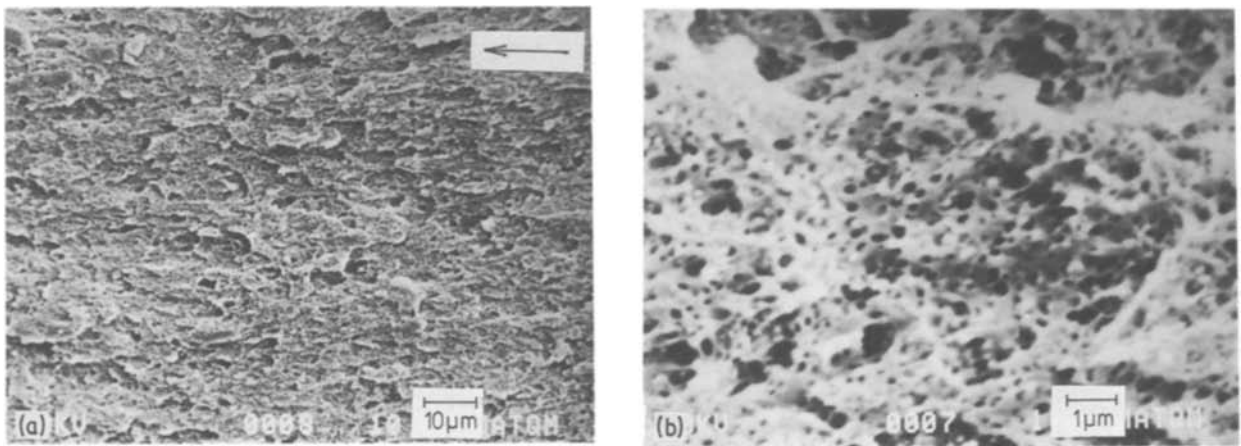


Figure 8 (a, b) Scanning electron micrographs of fracture surfaces produced by stable crack propagation for 0/20. The arrow shows the direction of crack propagation.

powder or alone, a substantial increase in elongation compared to standard bone cement was obtained, with a corresponding reduction in tensile modulus, yield stress and ultimate tensile strength. An increase in fracture toughness paralleled the increase in elongation to give bone cement values approaching those for cortical bone and bone analogue materials [2]. The increase in elongation with an increase in the rubber-

toughened PMMA powder to PMMA powder ratio may be attributed to the corresponding increase in the number of particle-filled as opposed to particle-free (PMMA powder) regions. Such a two-phase structure may be compared with the two phases of PMMA powder and PMMA matrix observed in standard bone cement [17–19], which has in turn a higher fracture toughness than homogeneous bulk-polymerized

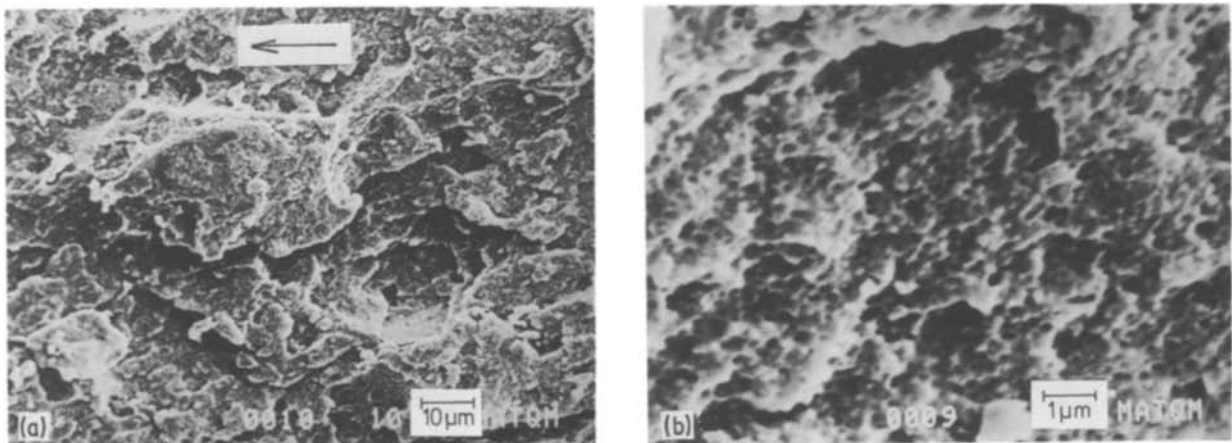


Figure 9 (a, b) Scanning electron micrographs of fracture surfaces produced by unstable crack propagation for 0/20. The arrow shows the direction of crack propagation.

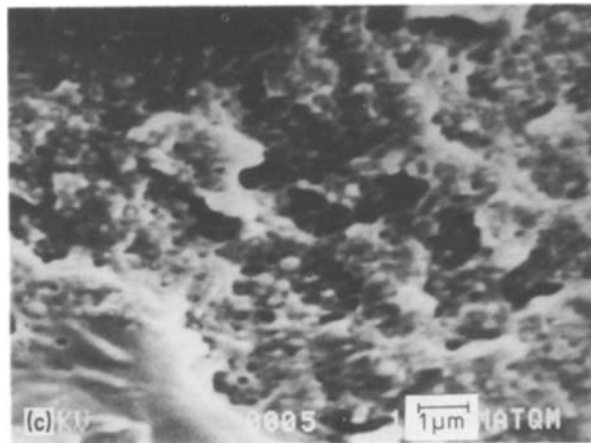
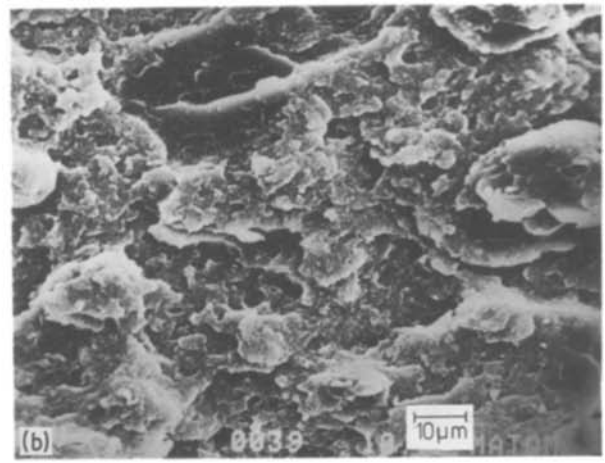
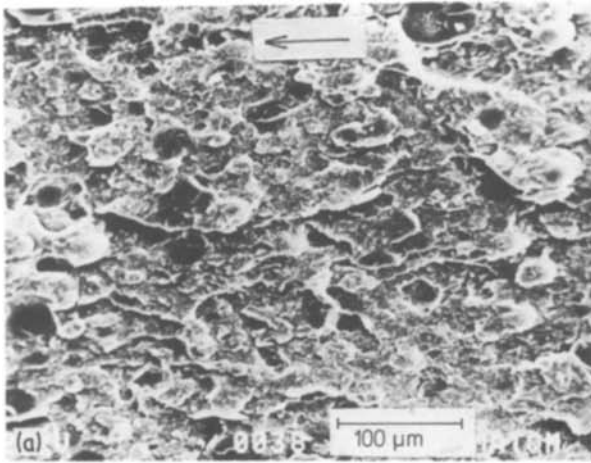


Figure 10 (a–c) Scanning electron micrographs of fracture surfaces produced by unstable crack propagation for 15/15. The arrow shows the direction of crack propagation.

PMMA [20]. The transition into a single-phase particle-filled matrix, as obtained by using rubber-toughened PMMA powder alone, provides a significant increase in elongation, but the effect of an increasing volume fraction of particles is not apparent. There is also a difference between the rubber-toughened PMMA–MMA monomer cements (Table III) and the “100%” rubber-toughened PMMA specimens (Table II), with the latter group having a reduced modulus, giving a consistent trend with increasing “rubber” content across the range of specimens, but comparable values of elongation and ultimate tensile strength. The increase in toughness

obtained in “bulk” rubber-toughened PMMA is generally associated with shear yielding and cavitation in the rubbery particles and debonding at the particle–matrix interface [7, 10, 21]. However, the results of this investigation suggest that crazing should also be considered [16] and this effect will be further studied. As the increase in toughness obtained by the incorporation of rubber-toughened PMMA into bone cement is also accompanied by a decrease in setting temperature and time, then the system offers considerable potential for addressing the major problems in current orthopaedic practice.

## 6. Conclusions

1. Rubber-toughened PMMA powder may be obtained by ball-milling without degrading the mechanical properties.

2. The modification of a standard bone cement, by incorporating either combinations of rubber-toughened PMMA and PMMA powders or rubber-toughened PMMA powder alone, increases the elongation and fracture toughness, with a reduced setting time.

3. The increase in toughness is demonstrated by stress whitening associated with plastic deformation.

## Acknowledgements

The award of a Visiting Fellowship by Monbusho (Japan) to one of the authors (A.M.), together with support from CMW Dentsply Ltd and ICI plc, are gratefully acknowledged.

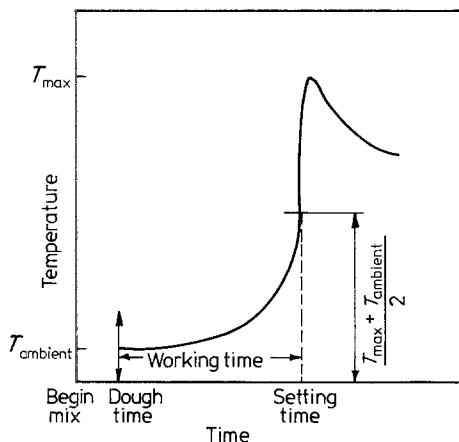


Figure 11 Schematic diagram of the curing characteristics of bone cement.

TABLE V Curing characteristics of bone cements

Material	Dough time (min)	Setting time (min)	$T_{max}$ (°C)
CMW	1 to 2	10 to 11	50.1
40/0	1 to 2	11 to 12	51.9
30/0	1 to 2	11 to 12	64.5
15/15	1 to 2	7 to 8	60.3
0/20	1 to 2	6 to 7	59.7

## References

1. J. CHARNLEY, "Acrylic Cement in Orthopaedic Surgery" (Livingstone, Edinburgh, 1970).
2. W. BONFIELD, in "Biocompatibility of Tissue Analogs", Vol. 2, edited by D. F. Williams (CRC Press, Boca Raton, Florida 1985) p. 89.
3. A. KNOELL, H. MAXWELL and C. BECHTOL, *Ann. Biomed. Eng.* **3** (1975) 225.
4. R. M. PILLIAR, R. BACKWELL, I. MACNAB and H. V. CAMERON, *J. Biomed. Mater. Res.* **10** (1976) 893.
5. T. M. WRIGHT and P. S. TRENT, *J. Mater. Sci.* **14** (1979) 503.
6. T. M. WRIGHT and R. P. ROBINSON, *ibid.* **17** (1982) 2463.
7. C. J. HOOLEY, D. R. MOORE, M. WHALE and M. J. WILLIAM, *Plast. Rubb. Process. Appl.* **1** (1981) 345.
8. C. B. BUCKNALL and A. MANCHETTI, *J. Appl. Polym. Sci.* **28** (1983) 2689.
9. C. B. BUCKNALL, I. K. PARTRIDGE and M. V. WARD, *J. Mater. Sci.* **19** (1984) 2064.
10. O. FRANK and J. LEHMAN, *Colloid Polym. Sci.* **264** (1986) 473.
11. J. MILIOS, G. C. PAPANICOLAOU and R. J. YOUNG, *J. Mater. Sci.* **21** (1986) 4281.
12. US Patent 1414 187 (1972).
13. C. B. BUCKNALL, "Toughened Plastics" (Applied Science, London, 1977).
14. H. D. MOSKOWITZ and D. T. TURNER, *J. Appl. Polym. Sci.* **18** (1974) 143.
15. C. B. BUCKNALL and R. R. SMITH, *Polymer* **6** (1965) 437.
16. C. B. BUCKNALL, D. CLAYTON and W. E. KEAST, *J. Polym. Sci.* **7** (1972) 1443.
17. P. W. R. BEAUMONT and R. J. YOUNG, *J. Biomed. Mater. Res.* **9** (1975) 423.
18. R. P. KUSY, J. R. MAHAN and D. T. TURNER, *ibid.* **10** (1976) 77.
19. G. M. BRAUER, D. J. TERMINI and G. DICKSON, *ibid.* **11** (1977) 577.
20. G. D. STAFFORD, R. HUGGETT and B. E. CAUSTON, *ibid.* **14** (1980) 359.
21. A. J. KINLOCK, S. J. SHAW and D. A. TOD, *Polymer* **24** (1983) 1341.

*Received 23 March  
and accepted 28 July 1987*